1521-0103/12/3423-816–826$25.00
THE JOURNAL OF PHARMACOLOGY AND EXPERIMENTAL THERAPEUTICS Vol. 342, No. 3

193003/3789525
JPET 342:816–826, 2012

15-Deoxy-$\Delta^{12,14}$-Prostaglandin J_2-Glycerol, a Putative Metabolite of 2-Arachidonyl Glycerol and a Peroxisome Proliferator-Activated Receptor γ Ligand, Modulates Nuclear Factor of Activated T Cells

Priyadarshini Raman, Barbara L. F. Kaplan, and Norbert E. Kaminski

Department of Pharmacology and Toxicology and the Center for Integrative Toxicology, Michigan State University, East Lansing, Michigan

Received March 1, 2012; accepted June 12, 2012

ABSTRACT

2-Arachidonyl glycerol (2-AG) is an endogenous arachidonic acid derivative released on demand from membrane precursors. 2-AG-mediated suppression of interleukin (IL)-2 depends on cyclooxygenase 2 (COX-2) metabolism and peroxisome proliferator-activated receptor γ (PPARγ) activation. 15-Deoxy-$\Delta^{12,14}$-prostaglandin J_2-glycerol ester (15d-PGJ_2-G), a putative COX-2 metabolite of 2-AG, acts as a PPARγ ligand and produces IL-2 suppression in activated Jurkat T cells, in part, by decreasing nuclear factor of activated T cells (NFAT) transcriptional activity. The objective of the present studies was to investigate the mechanism by which 15d-PGJ_2-G modulates NFAT activity to suppress IL-2. 15d-PGJ_2-G treatment decreased phorbol 12-myristate 13-acetate (PMA)/calcium ionophore (I_o)-induced NFAT DNA binding to the human IL-2 promoter and nuclear NFAT2 accumulation. It is noteworthy that 15d-PGJ_2-G treatment increased active nuclear HDM2 (human homolog of the oncoprotein and E3 ubiquitin ligase murine double minute 2) expression, whereas there was no change in the expression of glycogen synthase kinase 3β, both of which regulate NFAT. 15d-PGJ_2-G and other PPARγ agonists, such as rosiglitazone and ciglitazone, decreased PMA/I_o-mediated elevation in intracellular calcium concentration ($[Ca^{2+}]_i$) in activated Jurkat cells. We were surprised to find that the PPARγ antagonists 2-chloro-5-nitro-*N*-4-pyridinylbenzamide (T0070907) and 2-chloro-5-nitrobenzanilide (GW9662) also decreased the PMA/I_o-mediated elevation in $[Ca^{2+}]_i$ in activated T cells. In addition, the presence of T0070907 plus 15d-PGJ_2-G produced an additive decrease in PMA/I_o-mediated elevation of $[Ca^{2+}]_i$, suggesting that the 15d-PGJ_2-G effects on calcium might be either PPARγ-independent or -dependent on occupation of the PPARγ ligand binding domain. Collectively, our findings suggest that 15d-PGJ_2-G increases active nuclear HDM2, which could lead to a decrease in NFAT2 and IL-2 suppression.

Introduction

2-Arachidonyl glycerol (2-AG) is an arachidonic acid derivative that is released endogenously from membrane precursors on demand (Piomelli, 2003). 2-AG was first isolated from canine gut and found to bind both cannabinoid receptors as demonstrated in CB1- and CB2-transfected Chinese hamster ovary cells (Mechoulam et al., 1995; Sugiura et al., 1995); hence, it was termed an endocannabinoid. The immunomodulatory activities of 2-AG include suppression of cytokine production including tumor necrosis factor α release from lipopolysaccharide-treated murine macrophages and rat microglial cells and IL-6 production by J774 macrophages (Berdyshev, 2005). In T cells, 2-AG produced a concentration-dependent suppression of anti-CD3-induced T cell proliferation and the mixed lymphocyte response (Lee et al., 1995). In

This work was supported in part by the National Institutes of Health National Institute on Drug Abuse [Grant RO1-DA020402] and research fellowships from Pfizer Global Research and Development.
Article, publication date, and citation information can be found at http://jpet.aspetjournals.org.
http://dx.doi.org/10.1124/jpet.112.193003.

ABBREVIATIONS: 2-AG, 2-arachidonyl glycerol; 15d-PGJ_2-G, 15-deoxy-$\Delta^{12,14}$-prostaglandin J_2-glycerol ester; $[Ca^{2+}]_i$, intracellular calcium concentration; CB, cannabinoid receptor; CGZ, ciglitazone; CsA, cyclosporin A; EtOH, ethanol; GSK-3β, glycogen synthase kinase 3β; HDM2, human homolog of the oncoprotein and E3 ubiquitin ligase murine double minute 2; IL, interleukin; I_o, calcium ionophore; NA, naive; N:C, nuclear to cytoplasmic; NFAT, nuclear factor of activated T cells; PBS, phosphate-buffered saline; PMA, phorbol 12-myristate 13-acetate; PMSF, phenylmethylsulfonyl fluoride; PPARγ, peroxisome proliferator activated receptor γ; RGZ, rosiglitazone; RXR, retinoid X receptor; Th, T helper; VH, vehicle; GW9662, 2-chloro-5-nitrobenzanilide; T0070907, 2-chloro-5-nitro-*N*-4-pyridinylbenzamide; GI 262570, 2(*S*)-(2-benzoylphenylamino)-3-[4-[2-(5-methyl-2-phenyloxazol-4-yl)ethoxy]phenyl]propionic acid; GW 7845, (2*S*)-2-[(2-methoxycarbonylphenyl)amino]-3-[4-[2-(5-methyl-2-phenyl-1,3-oxazol-4-yl)ethoxy]phenyl]propanoic acid; GW 1929, *N*-(2-benzoylphenyl)-*O*-[2-(methyl-2-pyridinylamino)ethyl]-L-tyrosine.

addition, 2-AG suppressed IL-2 secretion in activated murine splenocytes (Ouyang et al., 1998) and Jurkat T cells (Rockwell et al., 2006) in part because of the impairment of NFAT. Although many of the effects of 2-AG depend on the cannabinoid receptors, 2-AG-mediated IL-2 suppression in activated murine splenocytes occurs independently of both CB1 and CB2 receptors and depends on cyclooxygenase-2 metabolism and PPARγ activation. It is noteworthy that 15-deoxy-$\Delta^{12,14}$-prostaglandin J_2-glycerol ester (15d-PGJ_2-G), a putative cyclooxygenase-2 metabolite of 2-AG (Raman et al., 2011), binds the ligand binding domain of PPARγ and increases PPARγ transcriptional activity (Raman et al., 2011).

PPARγ is a ligand-activated transcription factor that is predominantly localized to the nucleus, although cytosolic localization has also been reported (Kanunfre et al., 2004; von Knethen et al., 2007). PPARγ usually exists as a heterodimer with retinoid X receptor (RXR). When localized in the nucleus and in its resting state, the PPARγ/RXR complex is associated with the PPAR response elements in the regulatory regions of various target genes. In this state, PPARγ/RXR complex may or may not exist in association with corepressors depending on the promoter. Upon ligand binding PPARγ undergoes a confirmational change, and the dissociation of corepressors (if associated) occurs along with the recruitment of coactivators such as steroid receptor coactivator-1 and cAMP response element-binding protein binding protein/p300, which facilitate the integration of histone acetyl transferases and contribute to transcriptional activation of target genes (Glass and Rosenfeld, 2000). In addition to transactivation, ligand-activated PPARγ/RXR participates in transrepression by physical association with, and sequestration of, transcription factors including NFAT, nuclear factor of the κ-enhancer in B cells, and activator protein-1. This interaction with PPARγ can lead to the inhibition of sequestered transcription factor function and gene regulation (Ricote et al., 1998; Yang et al., 2000). It is noteworthy that, in addition to the activation of the receptor, PPARγ ligands lead to the ubiquitination of the receptor (Hauser et al., 2000). Although all three PPAR subtypes have been detected in various immune cell types, PPARγ1 expression has been detected in T cells, and its activation has been correlated with IL-2 suppression (Clark et al., 2000).

NFAT is a transcription factor that binds to the IL-2 promoter and is requisite for IL-2 gene transcription. One of the mechanisms controlling NFAT translocation into the nucleus is the level of intracellular calcium concentration ($[Ca^{2+}]_i$). Elevation of $[Ca^{2+}]_i$ activates the calcium-dependent phosphatase calcineurin. Activated calcineurin dephosphorylates cytosolic NFAT, and the dephosphorylation exposes the nuclear localization signal, thus facilitating the nuclear entry of NFAT (Crabtree and Olson, 2002). Although $[Ca^{2+}]_i$ levels control NFAT translocation into the nucleus, HDM2, the human homolog of the oncoprotein and E3 ubiquitin ligase murine double minute 2, has been reported to ubiquitinate NFAT. Phosphorylation of HDM2 by Akt has been implicated in the degradation of a number of proteins including NFAT (Yoeli-Lerner et al., 2005). In PMA/I_o-stimulated Jurkat cells, 15d-PGJ_2-G decreased PMA/I_o-mediated induction of NFAT transcriptional activity in transiently transfected Jurkat cells. In addition, the PPARγ antagonist 2-chloro-5-nitro-*N*-4-pyridinylbenzamide (T0070907) partially reversed the actions of 15d-PGJ_2-G on NFAT transcriptional activity (Raman et al., 2011). Moreover, 15d-PGJ_2-G suppressed IL-2 in a concentration- and time-dependent manner, which was also attenuated by T0070907 (Raman et al., 2011). Thus, the overall objective of the current studies was to understand the mechanisms by which 15d-PGJ_2-G decreases NFAT activity on the human IL-2 promoter. To address this objective, we investigated NFAT-DNA binding activity along with the roles of HDM2, GSK-3β, and $[Ca^{2+}]_i$ levels after 15d-PGJ_2-G treatment in activated Jurkat cells.

Materials and Methods

Reagents. Ciglitazone (CGZ), rosiglitazone (RGZ), 15d-PGJ_2-G, and 2-chloro-5-nitro-*N*-4-pyridinylbenzamide (T0070907) were purchased from Cayman Chemical (Ann Arbor, MI). All other reagents were purchased from Sigma-Aldrich (St. Louis, MO) unless otherwise indicated.

Animals and Cell Culture. Female B6C3F1 mice, 6 weeks of age, were purchased from Charles River Laboratories, Inc. (Wilmington, MA). Studies requiring animals were conducted in accordance with the *Guide for the Care and Use of Laboratory Animals* as adopted by the National Institutes of Health (Institute of Laboratory Animal Resources, 1996) and approved by the Institutional Animal Care and Use Committee at Michigan State University. Spleens were isolated aseptically and processed into single-cell suspensions (2×10^6 cells/ml) in RPMI 1640 medium supplemented with 2% bovine calf serum for calcium determination assays. Jurkat E6-1 T cells were purchased from the American Type Culture Collection (Manassas, VA). Jurkat cells were cultured in RPMI 1640 medium supplemented with 10% bovine calf serum, 100 units/ml penicillin, 100 μg/ml streptomycin, and 1× solutions of nonessential amino acids and sodium pyruvate (Invitrogen, Carlsbad, CA).

Electrophoretic Mobility-Shift Assays. Nuclear proteins were isolated from naive (NA) or PMA/I_o (40 nM/0.5 μM)-activated (for 30 min) Jurkat cells (2.5×10^7 cells/ml) that were pretreated with either vehicle (VH; 0.1% EtOH), 15d-PGJ_2-G (1, 5, and 10 μM), or cyclosporin A (CsA; 0.01 μM; used as a positive control) for 30 min. After the culture period, the cells were pelleted and washed once with cold 1× PBS. Then the cell pellets were resuspended in 5 ml of hypotonic buffer (10 mM HEPES, pH 7.5, 1.5 mM $MgCl_2$, 1 mM dithiothreitol, and 0.2 mM PMSF) and allowed to swell on ice for 15 min. The samples were then centrifuged at 3000 rpm for 5 min at 4°C, and the supernatants were discarded. The nuclear pellets were washed three times with 2 ml of MDHS buffer (3 mM $MgCl_2$, 25 mM HEPES, pH 7.5, 0.1M NaCl, 1 mM dithiothreitol, and 0.2 mM PMSF) and pelleted at 3000 rpm for 5 min at 4°C. The nuclear pellets were resuspended in 100 μl of cold buffer C (30 mM HEPES, pH 7.5, 1.5 mM $MgCl_2$, 0.3 mM EDTA, 0.45 mM NaCl, 0.1% Igepal, 1 mM dithiothreitol, and 0.2 mM PMSF) and rocked on ice for 30 min for high-salt extraction. Cellular debris was removed by centrifugation at 14,000 rpm for 15 min at 4°C. The supernatants were collected and combined with 100 μl of cold buffer D (30 mM HEPES, pH 7.5, 1.5 mM $MgCl_2$, 0.3 mM EDTA, 10% glycerol, 1 mM dithiothreitol, and 0.2 mM PMSF). The protein concentration of the supernatant was quantified by using the bicinchoninic acid assay (Sigma-Aldrich). The binding reaction was performed by adjusting the final NaCl concentration to 25 mM by the addition of buffer D (buffer C prepared as above, but devoid of NaCl) followed by incubation of 1 μg of nuclear protein with 62.5 ng of poly(deoxyinosinic-deoxycytidylic) acid (Roche Diagnostics, Indianapolis, IN) on ice for 10 min. After incubation with poly(deoxyinosinic-deoxycytidylic) acid, the double-stranded ^{32}P-labeled probe containing the NFAT site derived from human IL-2 promoter (5′-AGAAAGGAGGAAAAACTGTT-3′; 45,000 cpm per lane) (Badran et al., 2002) was added to the reaction and incubated at room temperature for another 20 min. To assess the specificity of DNA binding activity, the nuclear extracts were incubated with 100-fold excess of unlabeled probe before the addition of

the radiolabeled probe. The resulting protein-DNA complexes were resolved on a 4% polyacrylamide gel in 0.5× TBE buffer (89 mM Tris, 89 mM borate, and 2 mM EDTA). The gel was then dried on 3-mm filter paper (Whatman, Clifton, NJ) and autoradiographed. Autoradiograph bands were quantified by densitometry using the image-processing software ImageJ, version 10.2 (http://rsbweb.nih.gov/ij). For the supershift assay, the nuclear proteins were incubated with anti-NFATc1 monoclonal (7A6) antibody (Thermo Fisher Scientific, Waltham, MA) for 1 h at 4°C before the addition of radiolabeled probes.

Cellular Fractionation and Western Blotting. Naive or PMA/I_o-activated Jurkat cells (2.5×10^7 cells) pretreated with vehicle or 15d-PGJ_2-G (10 μM) were subjected to cellular fractionation by using the modified REAP method (Suzuki et al., 2010). In brief, after the culture period, the cells were harvested and the cell pellet was washed with 5 ml of ice-cold PBS. After the wash, the cells were pelleted and resuspended in 500 μl of buffer A (0.1% Igepal in 1× PBS, 1 mM dithiothreitol, and 0.2 mM PMSF), and the samples were triturated 10 times by using a p1000 micropipette. The samples were incubated on ice for 10 min and triturated again 10 times. An aliquot of the samples was observed under the compound microscope for the complete disruption of cell membranes and the presence of intact nuclei. The nuclei were pelleted by centrifuging for 10 s (short setting) in the microfuge. Three hundred microliters of the supernatant, containing the cytosolic fraction, was collected, and 100 μl of 4× loading buffer (0.25 M Tris, 8% SDS, 40% glycerol, 0.04% bromophenol blue, and 4% 2-mercaptoethanol) was added. The remaining supernatant was discarded, and the nuclear pellets were washed twice with ice-cold buffer A. The nuclear pellet was resuspended in 125 μl of 1× loading buffer (0.0625 M Tris, 2% SDS, 10% glycerol, 0.01% bromophenol blue, and 1% 2-mercaptoethanol) and sonicated by using microprobes at level 2, twice for 5 s. This resultant nuclear fraction was therefore four times more concentrated than the cytosolic fraction. Both the cytosolic and the nuclear fractions were boiled for 3 min at 95°C. Five microliters of the cytosolic fraction and 25 μl of the nuclear fraction were used for the detection of NFAT2, PPARγ, α-tubulin, and histone H1. Five microliters of the cytosolic fraction and 10 μl of the nuclear fraction were used for the detection of GSK-3β, phospho-GSK-3β, HDM2, and phospho-HDM2. The samples were loaded into SDS-polyacrylamide gels (7.5% for NFAT2, PPARγ, GSK3β, phospho-GSK3β, HDM2, and phospho-HDM2; 12% for α-tubulin and histone H1), transferred to a nitrocellulose membrane, and incubated with blocking buffer (5% dry nonfat milk in Tris-buffered saline containing 0.05% Tween 20). The following primary antibodies were used: NFAT2 (anti-NFATc1; Thermo Fisher Scientific), PPARγ (anti-PPARγ; Santa Cruz Biotechnology Inc., Santa Cruz, CA), GSK-3β (anti-GSK-3β; Cell Signaling Technology, Danvers, MA), phospho-GSK-3β [antiphospho-GSK-3β (Ser9); Cell Signaling Technology], HDM2 (anti-HDM2-323; Santa Cruz Biotechnology Inc.), phospho-HDM2 [antiphospho-HDM2 (Ser166); Santa Cruz Biotechnology Inc.], α-tubulin (antitubulin-α; BioLegend, San Diego, CA), and histone H1 (antihistone H1; Santa Cruz Biotechnology Inc.). Secondary antibodies were horseradish peroxidase-linked (GE Healthcare, Chalfont St. Giles, Buckinghamshire, UK). The blots were developed by using Supersignal West Femto maximum sensitivity substrate (Thermo Fisher Scientific). Bands were quantified by densitometry using the image-processing software ImageJ, version 10.2 (http://rsbweb.nih.gov/ij). Bands were first normalized to the respective loading controls, and fold change was calculated compared with the naive control within each fraction.

Calcium Determination. Jurkat cells and splenocytes were discriminated by flow cytometric measurements of cellular forward scatter and right angle scatters, using a FACScalibur (BD Biosciences, San Jose, CA). Fluo3 (Invitrogen) and Fura Red (Invitrogen) were excited at 488 nm. Fluo3 emission was detected at 530/30 nm, and Fura Red emission was detected at 670/LP nm. For experiments involving the addition of only the PPARγ agonists, the first 1 min of the analysis was considered as an initial baseline. Then, the VH/PPARγ agonist was added for a min followed by the addition of PMA/I_o (40 nM/0.5 μM), and the measurement was continued for another 3 min. For experiments involving the addition of PPARγ antagonists, the first 1 min of the analysis was considered as an initial baseline. At the end of 1 min, the VH/PPARγ antagonist was added. After another minute, VH/PPARγ agonist was added for 1 min. Then, PMA/I_o (40 nM/0.5 μM) was added, and the measurement was continued for another 3 min. For all experiments, the ratio intensity of Fluo3/Fura Red versus time was calculated by using FlowJo (Tree Star Inc., Ashland, OR).

Statistical Analysis. The mean ± S.E. was determined for each treatment group in the individual experiments. Homogenous data were evaluated by one-way parametric analysis of variance. Dunnett's two-tailed *t* test was used to compare treatment groups with the vehicle control when significant differences were observed by using Prism software (GraphPad Software, Inc., San Diego, CA).

Results

15d-PGJ_2-G Decreased NFAT-DNA Binding Activity in Activated Jurkat Cells. Because of our previous finding that 15d-PGJ_2-G decreased IL-2 secretion and NFAT transcriptional activity in activated Jurkat cells (Raman et al., 2011), the effect of 15d-PGJ_2-G on NFAT-DNA binding in activated Jurkat cells was investigated. An NFAT oligonucleotide derived from the human IL-2 promoter was used for the electrophoretic mobility-shift assay. Three NFAT-DNA complexes were detected upon autoradiography (Fig. 1). Cell stimulation by PMA/I_o for 30 min (Fig. 1, lane 3) increased NFAT-DNA binding activity compared with resting cells (naive; Fig. 1, lane 2). VH treatment (Fig. 1, lane 4) did not alter the PMA/I_o-stimulated NFAT-DNA binding activity. Pretreatment with 15d-PGJ_2-G (1, 5, and 10 μM; Fig. 1, lanes 5–7) followed by PMA/I_o stimulation decreased NFAT-DNA binding activity. In the presence of a cold competitor (100-fold molar excess; Fig. 1, lane 8) in the binding reaction, all three bands corresponding to NFAT-DNA complexes disappeared, indicating specificity. CsA, a specific inhibitor of NFAT activity (Clipstone and Crabtree, 1992), impaired PMA/I_o-induced NFAT-DNA binding activity as expected. To confirm the identity of the observed NFAT-DNA complexes, a super-shift assay was performed. When the PMA/I_o-stimulated sample was preincubated with anti-NFAT2 antibody (2 and 1 μg; Fig. 1), there was a shift in the lower band, and the upper and middle bands intensified, confirming that the detected complexes contain NFAT2.

Decreased NFAT2 and PPARγ Nuclear Localization by 15d-PGJ_2-G Treatment of Activated Jurkat Cells. Based on the decrease in NFAT-DNA binding activity after 15d-PGJ_2-G treatment, NFAT2 localization was further investigated. The localization of PPARγ was also investigated because 15d-PGJ_2-G acts as a ligand for PPARγ (Raman et al., 2011). α-Tubulin was used as the cytosolic loading control, and histone H1 was used as the nuclear loading control. The mutually exclusive identification of α-tubulin and histone H1 in cytosolic and nuclear fractions, respectively, suggests there was minimal cross-contamination between the two cellular compartments. Ponceau staining of bands corresponding to histone exclusively in the nuclear fraction further suggest the same. Concerning NFAT2 localization, there were modest levels of NFAT2 in the nucleus and high expression of NFAT2 in the cytosol of resting cells (NA). Upon activation, nuclear NFAT2 in-

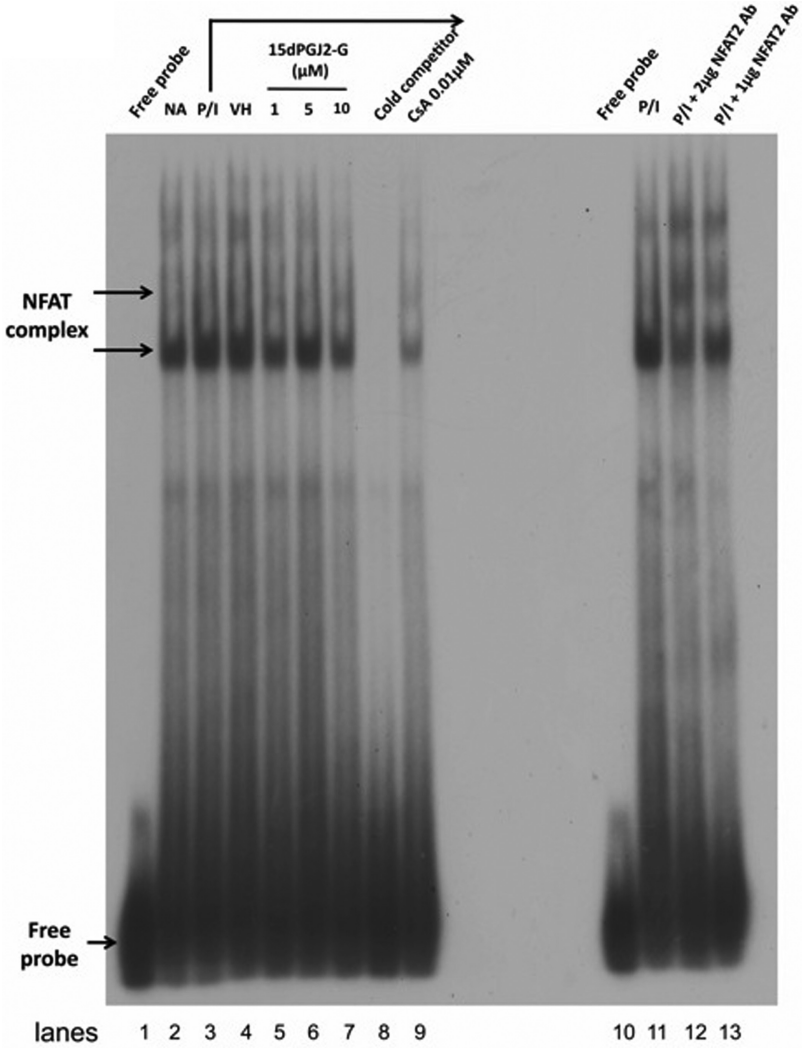

Fig. 1. NFAT2 DNA binding activity at human IL-2 promoter in activated Jurkat cells when treated with 15d-PGJ_2-G. Jurkat cells (2.5×10^7) were pretreated with VH (0.1% EtOH; lane 4), 15d-PGJ_2-G (1, 5 and 10 μM; lanes 5, 6, and 7, respectively), or CsA (0.01 μM; lane 9) for 30 min and then stimulated with PMA/I_o (40 nM/0.5 μM) for 30 min at 37°C. In addition, the basal level of NFAT DNA binding was measured in unstimulated cells (lane 2). The nuclear proteins (1 μg) were resolved by electrophoretic mobility-shift assay as described under *Materials and Methods*. Arrows, NFAT/DNA complex or free probe. Lane 1, radiolabeled probe alone; lane 3, PMA/I_o-treated cells; lane 9, included 100-fold molar excess of the unlabeled NFAT oligonucleotide as a competitor using the same protein as loaded in lane 3. Lanes 10 to 13, supershift analysis of NFAT-DNA binding activity at human IL-2 promoter; lane 10, radiolabeled probe alone; lane 11, PMA/I_o-treated cells; lanes 12 and 13, preincubated anti-NFAT2 antibody (2 and 1 μg, respectively) for 1 h along with the same protein as loaded in lane 11. The data are representative of three independent experiments.

creased with a corresponding decrease in cytosolic NFAT2. Pretreatment with VH followed by activation did not significantly alter the increase in nuclear NFAT2 or the corresponding decrease in cytosolic NFAT2 (Fig. 2, A and B). Upon pretreatment with 15dPGJ_2-G followed by PMA/I_o activation, there was a significant decrease in the nuclear and cytosolic NFAT2 (Fig. 2, A and B). In resting cells (NA) PPARγ was localized predominantly in the cytosol compared with the nucleus (Fig. 2A). It is noteworthy that 20 times more protein was loaded per lane in the nuclear fraction determinations than for cytosolic determinations. PMA/I_o stimulation alone or VH treatment followed by PMA/I_o stimulation did not significantly alter the PPARγ localization either in the nucleus or the cytosol (Fig. 2, A and C). When Jurkat cells were treated with 15d-PGJ_2-G before activation with PMA/I_o, there was a decrease in the localization of PPARγ in both the nuclear and the cytosolic fractions (Fig. 2, A and C).

15d-PGJ_2-G Did Not Change the Levels of the Active Form of GSK-3β in Activated Jurkat Cells. Expression levels of total GSK-3β and phospho-GSK-3β (inactive form) were investigated to understand whether GSK-3β was responsible for the observed decrease in nuclear NFAT2 accumulation in activated Jurkat cells pretreated with 15d-PGJ_2-G (Fig. 2, A and C). Active GSK-3β acts as a maintenance kinase (retains phosphorylated NFAT in the cytosol), as well as an export kinase (phosphorylates NFAT in the nucleus, causing its export). In resting cells (NA), there was very little inactive GSK-3β (phospho-GSK-3β) in the nucleus, suggesting that GSK-3β was predominantly in the active form, thus facilitating NFAT2 export to the cytosol (Figs. 2A and 3, A and B). Upon cellular activation, there was an increase in the inactive GSK-3β (phospho-GSK-3β) in the nucleus, suggesting that there was a decrease in the active GSK-3β, facilitating NFAT2 accumulation in the nucleus (Figs. 2A and 3, A and B). Pretreatment with VH or 15d-PGJ_2-G (J2G) followed by PMA/I_o activation did not significantly alter the expression of either total GSK-3β or phospho-GSK-3β, suggesting that there was no change in active GSK-3β compared with PMA/I_o-treated cells (Fig. 3, A and B). In addition, the nuclear to cytoplasmic (N:C) ratio of total GSK-3β and phospho-GSK-3β did not change with 15d-PGJ_2-G treatment (Fig. 3C).

15d-PGJ_2-G Increased the Nuclear Levels of Total HDM2 and Active Form of HDM2 in Activated Jurkat Cells. The observed decrease by 15d-PGJ_2-G on nuclear and cytosolic NFAT2 levels in activated T cells could not be attributed to changes in the nuclear or cytosolic expression of GSK-3β, one of the important kinases that regulates nuclear NFAT accumulation. Hence an alternative mechanism, the

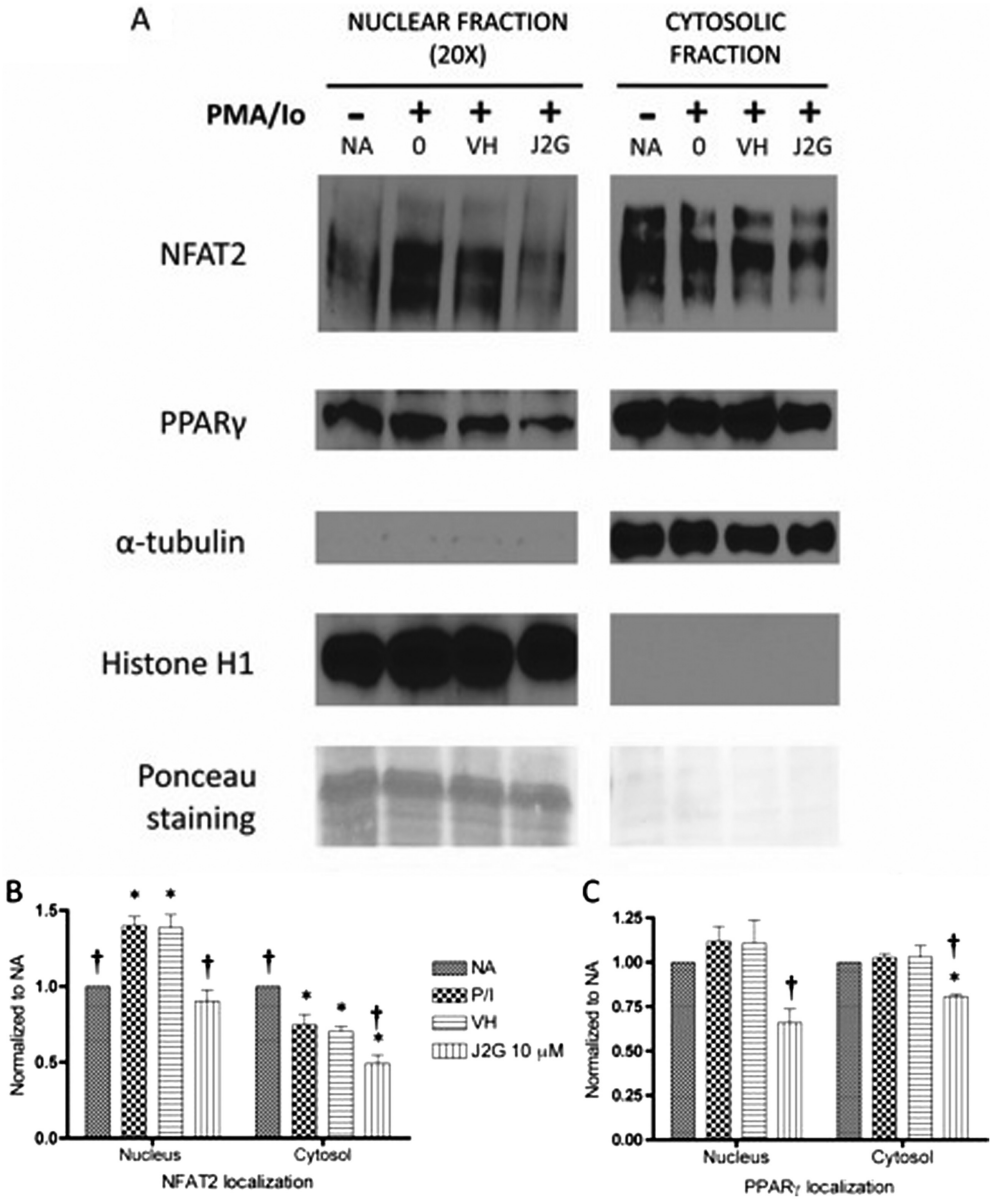

Fig. 2. Western blot analysis of NFAT2 and PPARγ protein levels in resting and activated Jurkat T cells pretreated with 15d-PGJ_2-G. Jurkat T cells were either left untreated (NA) or treated with VH (0.1% EtOH) or 15d-PGJ_2-G (J2G 10 μM) for 30 min followed by treatment with PMA/I_o (40 nM/0.5 μM) for 30 min. A, the nuclear and cytosolic fractions from these treatment groups were obtained and analyzed by Western blotting. α-Tubulin was used a loading control for cytosolic fraction, and histone H1 was used as a loading control for nuclear fraction. In addition, ponceau staining (corresponding to histone bands) also suggested very little cross-contamination between the fractions. B and C, NFAT2 protein levels (B) and PPARγ protein levels (C) within each fraction were quantified by densitometric analysis and normalized to the loading controls (α-tubulin and histone H1). The normalized results are expressed as fold change compared with NA within each fraction. Statistical analysis was performed by using Dunnett's test for each fraction. *, $p < 0.05$ compared with NA within the respective fraction. †, $p < 0.05$ compared with VH within the respective fraction. The data are representative of three independent experiments.

role of 15d-PGJ_2-G-induced ubiquitination of NFAT2, was investigated. The expression levels of both total HDM2 and phospho-HDM2 (active form) were assessed because active HDM2 (E3 ubiquitin ligase) has been implicated in the ubiquitination of NFAT (Yoeli-Lerner et al., 2005) (Fig. 4A). The expression of total HDM2 and active HDM2 (phospho form) was increased in the nucleus with a corresponding decrease in the cytosol upon 15d-PGJ_2-G pretreatment followed by PMA/I_o-induced activation (Fig. 4, A and B). This increase in the total and active HDM2 in the nucleus was further evident with the N:C ratio, suggesting that there was increased active HDM2 in the nucleus of activated Jurkat cells treated with 15d-PGJ_2-G (Fig. 4C). This increased expression of HDM2 might be responsible for the ubiquitination of NFAT2, potentially leading to decreased localization of NFAT2 in the nucleus of 15d-PGJ_2-G-treated, PMA/I_o-stimulated cells (Fig. 2A).

15d-PGJ_2-G and PPARγ Antagonists Decreased PMA/I_o-Induced Elevation in $[Ca^{2+}]_i$ in Activated Jurkat Cells. Because changes in the level of $[Ca^{2+}]_i$ (by regulating calcineurin activation) contribute to the mechanism by which NFAT translocation into the nucleus is modulated, the effect of 15d-PGJ_2-G on PMA/I_o-induced elevation in $[Ca^{2+}]_i$ in activated Jurkat cells was investigated. 15d-PGJ_2-G decreased PMA/I_o-induced elevation in $[Ca^{2+}]_i$ (Fig. 5A). 15d-PGJ_2-G also decreased PMA/I_o-induced elevation in $[Ca^{2+}]_i$ in mouse splenocytes, (Fig. 5B), and although the PMA/I_o-induced elevation in $[Ca^{2+}]_i$ in splenocytes did not return to baseline as it did in Jurkat cells, the effect of 15d-PGJ_2-G on $[Ca^{2+}]_i$ was confirmed. Two well studied PPARγ agonists, CGZ and RGZ, also decreased PMA/I_o-induced elevation in $[Ca^{2+}]_i$ in activated Jurkat cells (Fig. 6). Because 15d-PGJ_2-G and the other known PPARγ agonists such as RGZ and CGZ decreased $[Ca^{2+}]_i$ in PMA/I_o-activated Jurkat cells, we investigated whether this decrease depended on PPARγ by using two different PPARγ antagonists, T0070907 and 2-chloro-5-nitrobenzanilide (GW9662). We were surprised to find that both T0070907 and GW9662 alone decreased PMA/I_o-mediated elevation in $[Ca^{2+}]_i$ in activated Jurkat cells

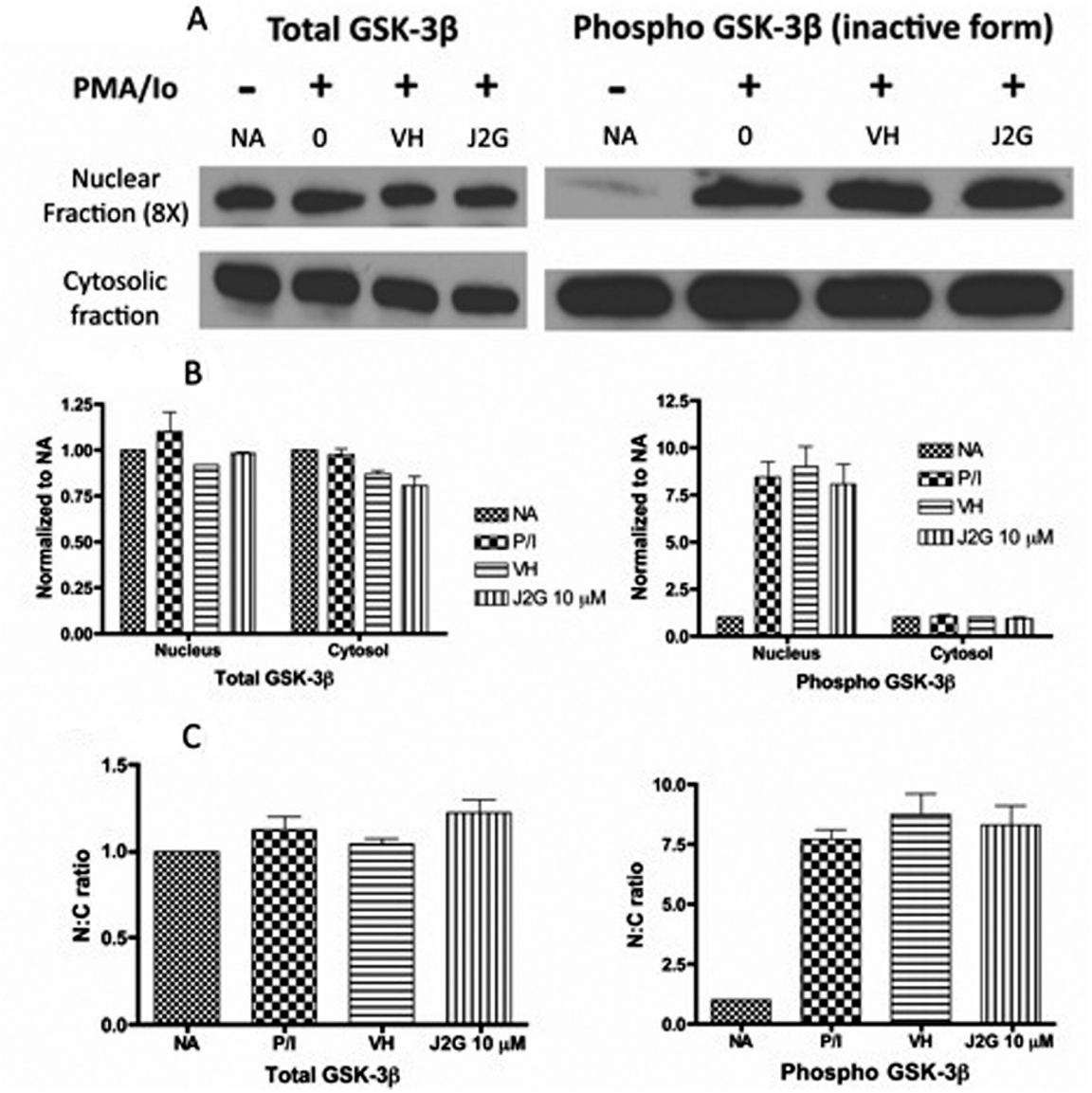

Fig. 3. Western blot analysis of total GSK-3β and phospho-GSK-3β protein levels in resting and activated Jurkat T cells pretreated with 15d-PGJ_2-G. Jurkat T cells were either left untreated (NA) or treated with VH (0.1% EtOH) or 15d-PGJ_2-G (J2G 10 μM) for 30 min followed by treatment with PMA/I_o (40 nM/0.5 μM) for 30 min. A, the nuclear and cytosolic fractions from these treatment groups were obtained and analyzed by Western blotting. α-Tubulin (from Fig. 2) was used a loading control for cytosolic fraction and histone H1 (from Fig. 2) was used as a loading control for nuclear fraction. B, total GSK-3β (left) and phospho-GSK-3β (right) protein levels within each fraction were quantified by densitometric analysis and normalized to the loading controls (α-tubulin and histone H1). The normalized results are expressed as fold change compared with NA within each fraction. C, the N:C ratio of total GSK-3β (left) and phospho-GSK-3β (right) was calculated. The data are representative of two independent experiments.

(Fig. 7, A and B). In addition, when activated Jurkat cells were pretreated with both T0070907 and 15d-PGJ_2-G there was an additive effect (decrease in $[Ca^{2+}]_i$ caused by both antagonists and agonists) on the decrease in PMA/I_o-mediated elevation in $[Ca^{2+}]_i$ (Fig. 7C).

Discussion

The major objective of the current studies was to investigate the underlying mechanism responsible for decreased NFAT transcriptional activity produced by 15d-PGJ_2-G in activated T cells. It was evident that 15d-PGJ_2-G decreased NFAT-DNA binding activity in the human IL-2 promoter in activated Jurkat cells, which probably contributed to attenuated IL-2 production (Raman et al., 2011). With 15d-PGJ_2-G treatment, there was a decrease in PMA/I_o-induced NFAT2 accumulation in both the nucleus and cytoplasm, suggesting that impairment of NFAT2 localization in the nucleus may also contribute to the 15d-PGJ_2-G-mediated suppression in IL-2 secretion. The decreased NFAT2 accumulation in the nucleus with 15d-PGJ_2-G treatment followed by PMA/I_o stimulation could be caused by either 1) decreased NFAT2 translocation into the nucleus, or 2) another mechanism such as ubiquitination that contributes to the decreased NFAT2 accumulation in both the nucleus and cytoplasm.

GSK-3β is a maintenance kinase that controls NFAT nuclear export by regulating the phosphorylation state of NFAT (Crabtree and Olson, 2002), but there were no significant changes in the expression of total and inactive GSK-3β comparing cells activated in the presence and

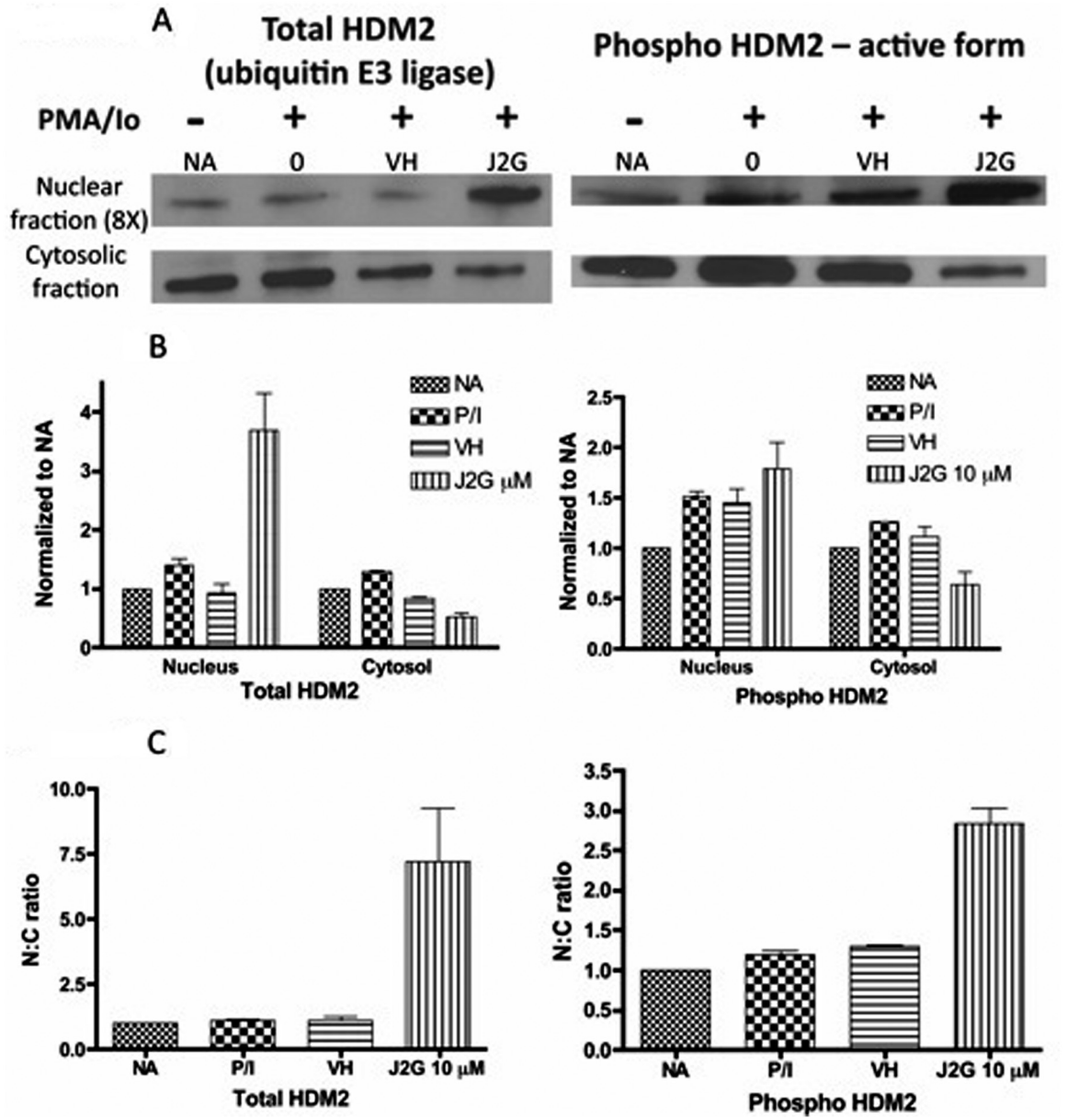

Fig. 4. Western blot analysis of total HDM2 and phospho-HDM2 protein levels in resting and activated Jurkat T cells pretreated with 15d-PGJ_2-G. Jurkat T cells were either untreated (NA) or treated with VH (0.1% EtOH) or 15d-PGJ_2-G (J2G 10 μM) for 30 min followed by treatment with PMA/I_o (40 nM/0.5 μM) for 30 min. A, the nuclear and cytosolic fractions from these treatment groups were obtained and analyzed by Western blotting. α-Tubulin (from Fig. 2) was used a loading control for cytosolic fraction and histone H1 (from Fig. 2) was used as a loading control for nuclear fraction. B, total HDM2 (left) and phospho-HDM2 (right) protein levels within each fraction were quantified by densitometric analysis and normalized to the loading controls (α-tubulin and histone H1). The normalized results are expressed as fold change compared with NA within each fraction. C, the N:C ratio of total HDM2 (left) and phospho-HDM2 (right) was calculated. The data are representative of two independent experiments.

absence of 15d-PGJ_2-G. These results are consistent with the localization patterns of nuclear and cytosolic NFAT2. The localization of NFAT2 in both the nucleus and cytosol was decreased, suggesting that GSK-3β is not involved, because a corresponding increase in cytosolic NFAT2 was not observed with the decreased nuclear NFAT2. Because a role for GSK-3β was ruled out in the decreased nuclear NFAT2 accumulation after 15d-PGJ_2-G treatment, the role of HDM2 (an ubiquitin E3 ligase) was investigated, which could better explain why NFAT2 expression was decreased in both the nucleus and cytoplasm upon 15d-PGJ_2-G treatment of activated Jurkat cells. Phosphorylation of HDM2 has been implicated in the ubiquitination of NFAT (Feng et al., 2004; Yoeli-Lerner et al., 2005). When PMA/I_o-activated Jurkat cells were treated with 15d-PGJ_2-G, there was an increase in both total HDM2 and phospho-HDM2 (active form) in the nucleus. This increase in active HDM2 may be responsible for the ubiquitination of NFAT2 in the nucleus, and once NFAT2 is exported into the cytosol, it can be degraded by cytosolic proteasomes.

Because 15d-PGJ_2-G acts as a PPARγ ligand (Raman et al., 2011), the effect of receptor activation on PPARγ localization was investigated. We were surprised to find that in Jurkat cells PPARγ was localized predominantly in the

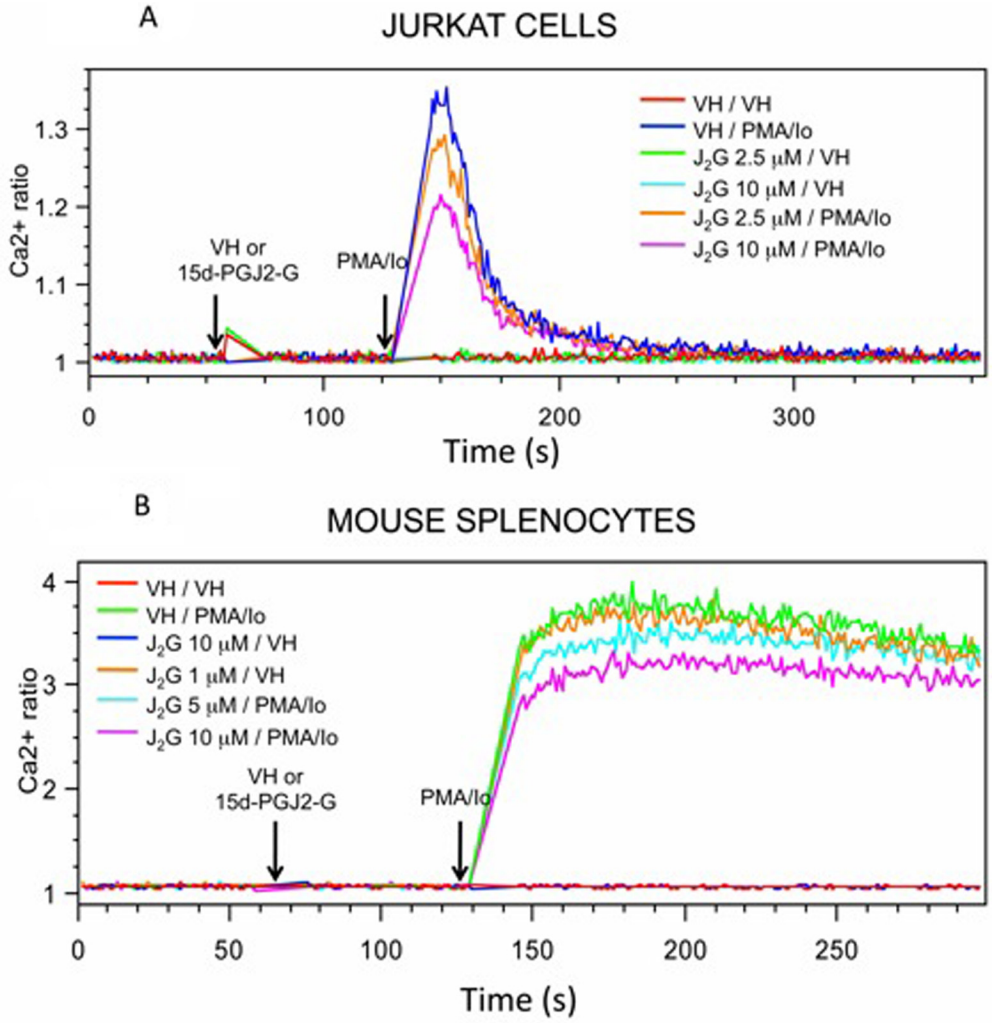

Fig. 5. The effect of 15d-PGJ_2-G on PMA/I_o-mediated increase in $[Ca^{2+}]_i$ in Jurkat cells (A) and B6C3F1 splenocytes (B). A 500-μl aliquot of Fura Red- and Fluo3-loaded cells (2×10^6 cells/ml) was treated with VH (0.1% EtOH) or 15d-PGJ_2-G at 60 s. PMA/I_o (40 nM/0.5 μM) was added at 135 s, and the $[Ca^{2+}]_i$ was measured up to 360 s. Arrows indicate the addition of PPARγ ligands and PMA/I_o. $[Ca^{2+}]_i$ changes are presented as the ratio intensity of Fluo3/Fura Red versus time. The calcium traces are representative of three independent experiments.

cytosolic fraction compared with the nuclear fraction. It is noteworthy that for Western blotting the nuclear fraction was loaded at a much higher concentration (approximately 20 times more protein) than the cytosolic fraction. Although PPARγ has been reported as being predominantly localized to the nucleus, there is an earlier report describing PPARγ in Jurkat cells as being predominantly a cytosolic protein (Kanunfre et al., 2004). In addition to receptor activation, PPARγ ligands led to receptor ubiquitination (Hauser et al., 2000). Because ligand-activated PPARγ has been previously found to interact with NFAT (Yang et al., 2000), it is possible that 15d-PGJ_2-G-activated PPARγ associates with NFAT, eventually leading to the degradation of both PPARγ and NFAT. Considering the expression patterns of HDM2 and GSK-3β, it is tempting to speculate that 15d-PGJ_2-G-mediated PPARγ activation primarily causes an increase in the expression of active HDM2 (E3 ubiquitin ligase) without a significant change in the expression of GSK-3β, resulting in ubiquitin tagging of PPARγ and/or PPARγ/NFAT complex formation, eventually leading to the degradation of both PPARγ and NFAT.

In addition to the above-mentioned mechanism, we examined the effect of 15d-PGJ_2-G on PMA/I_o-mediated increase in $[Ca^{2+}]_i$ in activated Jurkat cells because calcium levels can modulate calcineurin, a calcium-dependent phosphatase that regulates NFAT translocation into the nucleus (Clipstone and Crabtree, 1992). Interestingly, all five PPARγ ligands (PPARγ agonists 15d-PGJ_2-G, RGZ, and CGZ, and PPARγ antagonists T0070907 and GW9662) decreased PMA/I_o-mediated elevation in $[Ca^{2+}]_i$, suggesting either a PPARγ-independent mechanism or occupation of the PPARγ ligand binding domain, regardless of whether by an agonist or antagonist, causes a conformational change allowing PPARγ to couple with calcium channels. The predominance of PPARγ in the cytosol in Jurkat cells certainly increases the likelihood for PPARγ to couple with a calcium channel. Pioglitazone and other nonthiazolidinedione PPARγ agonists such as 2(*S*)-(2-benzoylphenylamino)-3-[4-[2-(5-methyl-2-phenyloxazol-4-yl)ethoxy]phenyl]propionic acid (GI 262570), (2*S*)-2-[(2-methoxycarbonylphenyl)amino]-3-*N*-(2-benzoylphenyl)-*O*-[2-(methyl-2-pyridinylamino)ethyl]-L-tyrosine (GW 1929) all have been reported to inhibit L-type voltage-dependent calcium channels in freshly isolated smooth muscle cells from mesenteric arteries and cause a decrease in $[Ca^{2+}]_i$ (Heppner et al., 2005). Rosiglitazone has also been demonstrated to decrease voltage-gated calcium channel currents in primary hippocampal cultured neurons (Pancani et al., 2009). Finally, rosiglitazone has been reported to decrease collagen-stimulated peak $[Ca^{2+}]_i$ concentrations in human platelets (which lack nuclei), indicating that PPARγ possesses nongenomic functions in addition to the well studied genomic functions (Moraes et al., 2010). These observations suggest that the

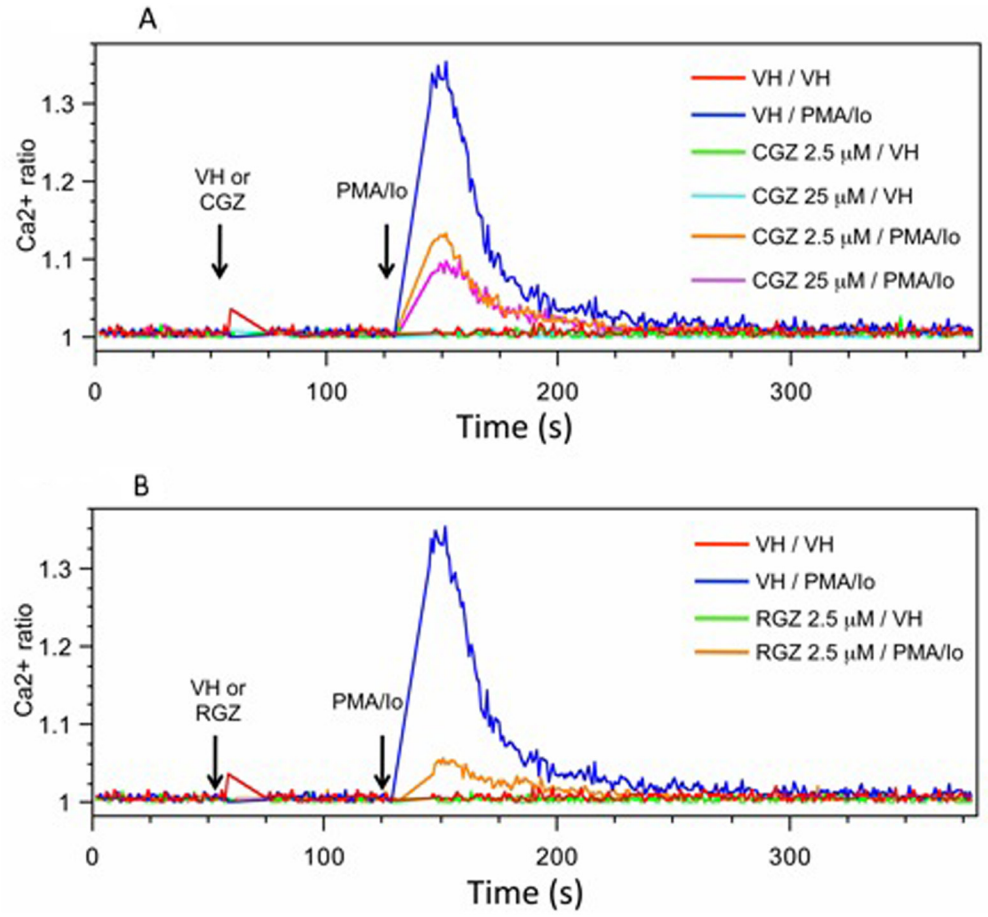

Fig. 6. The effect of CGZ and RGZ on PMA/I_o-mediated increase in $[Ca^{2+}]_i$ in Jurkat cells. A 500-μl aliquot of Fura Red- and Fluo3-loaded Jurkat cells (2×10^6 cells/ml) was treated with VH (0.1% EtOH) and CGZ (2.5 and 25 μM) (A) or RGZ (2.5 μM) (B) at 60 s. PMA/I_o (40 nM/0.5 μM) was added at 135 s, and the $[Ca^{2+}]_i$ was measured up to 360 s. $[Ca^{2+}]_i$ changes are presented as the ratio intensity of Fluo3/Fura Red versus time. The calcium traces are representative of three independent experiments.

decrease in $[Ca^{2+}]_i$ may be mediated, in part, through the action of PPARγ. Additional investigation is required to determine which types of calcium channels are modulated by PPARγ ligands.

Although the contribution of PPARγ to the decrease in $[Ca^{2+}]_i$ is unclear, the 15d-PGJ_2-G-mediated decrease in NFAT transcriptional activity depends on PPARγ as evidenced by the reversal of the decrease in NFAT transcriptional activity in the presence of a PPARγ antagonist, T0070907 (Raman et al., 2011). In addition, 15d-PGJ_2-G-mediated IL-2 suppression in activated Jurkat cells was attenuated in the presence of the PPARγ antagonist T0070907, although the reversal of IL-2 suppression was partial (Raman et al., 2011). The absence of complete reversal may be because T0070907 alone decreases $[Ca^{2+}]_i$ significantly, and, in the presence of 15d-PGJ_2-G, there is an additive decrease in $[Ca^{2+}]_i$. The partial attenuation of 15d-PGJ_2-G-mediated IL-2 suppression by a PPARγ antagonist could be a net effect of the following: 1) PPARγ antagonism on 15d-PGJ_2-G-mediated decrease in nuclear NFAT accumulation (via active HDM2), leading to an increase in nuclear NFAT, and 2) T0070907-mediated decrease in $[Ca^{2+}]_i$, leading to decreased nuclear NFAT.

In addition to IL-2 suppression, PPARγ has been shown to suppress the expression of proinflammatory cytokines such as tumor necrosis factor α, interleukin-1β, and interleukin-6 (Pascual and Glass, 2006; Széles et al., 2007). Furthermore, PPARγ ligands can inhibit activation-induced production of the classic Th1 cell cytokine, interferon γ, and IL-12 by dendritic cells (Cunard et al., 2002; Klotz et al., 2007), thus indicating that PPARγ might play a role during differentiation of naive T cells into their effector subsets. In addition, PPARγ blocks transforming growth factor-β/IL-6-dependent expression of the retinoid receptor-related orphan receptor γt, the key transcription factor for Th17 differentiation (Klotz et al., 2007). Hence, PPARγ is a promising molecular target for precise immune intervention in Th17-mediated autoimmune diseases such as multiple sclerosis. Identification of the molecular mechanisms responsible for the anti-inflammatory actions of PPARγ is therefore likely to be of practical importance in the efforts to develop effective and safer treatment options for diseases associated with autoimmunity.

It has been demonstrated that 2-AG levels are elevated in various immune cell types upon activation, and PPARγ activation and 2-AG and 15d-PGJ_2 (a known endogenous PPARγ ligand) treatments ameliorate the symptoms of numerous animal models of autoimmune diseases. Collectively, this suggests that activation of PPARγ by 15d-PGJ_2-G may play a significant role in the control of exaggerated immune responses through diminished NFAT signaling, thereby facilitating immune homeostasis. Therefore, 2-AG and its putative metabolite, 15d-PGJ_2-G, play an important role in maintaining immune homeostasis. Understanding the molecular targets involved in this immune homeostasis can help in developing a therapy directed to decrease exaggerated immune responses in autoimmune diseases.

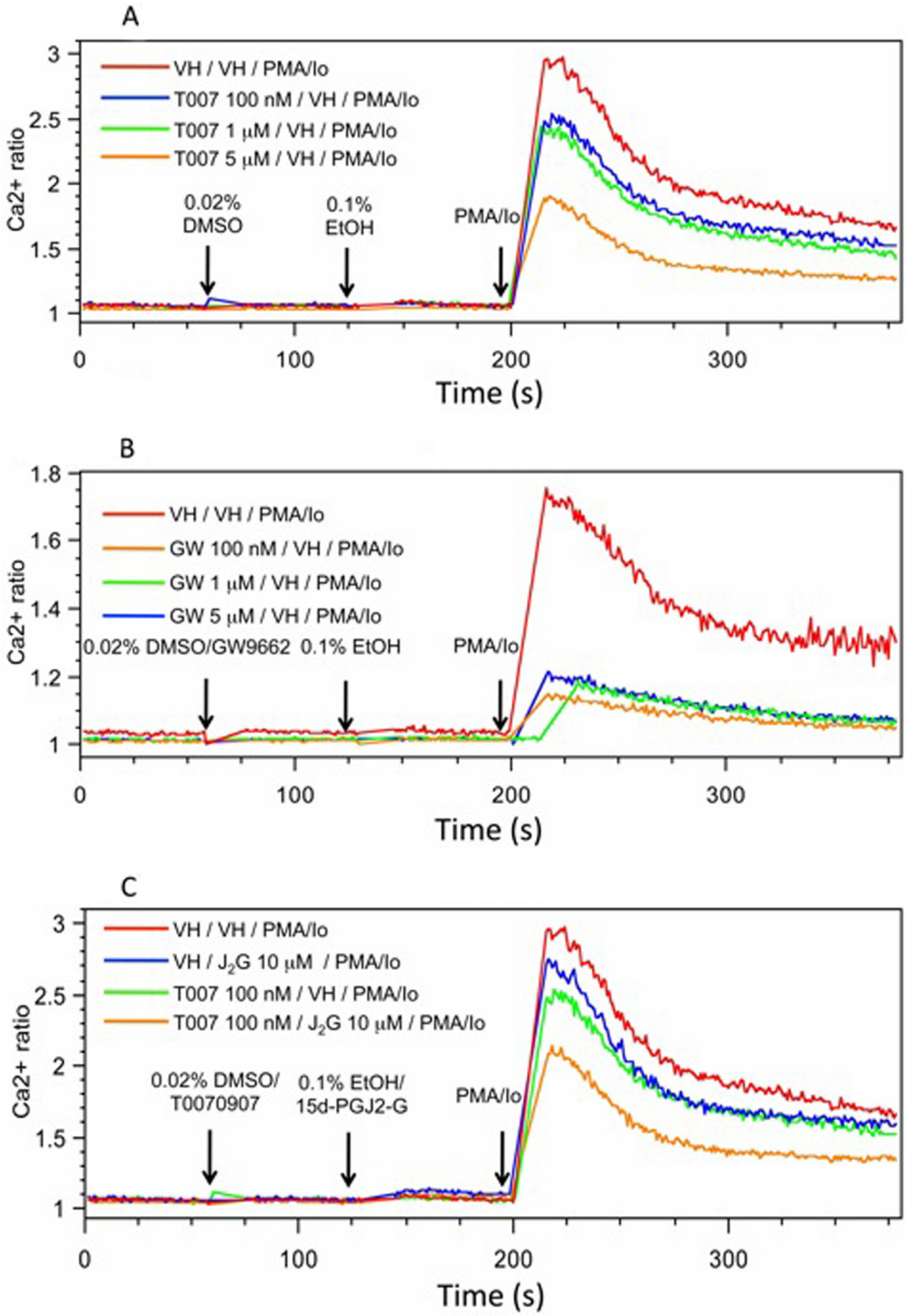

Fig. 7. The effect of T00709707 (A) and GW9662 (B) on PMA/I_o-mediated increase in $[Ca^{2+}]_i$ in Jurkat cells, and the effect of T0070907 on 15d-PGJ_2-G-mediated decrease in PMA/I_o-activated Jurkat cells (C). A 500-μl aliquot of Fura Red- and Fluo3-loaded Jurkat cells (2×10^6 cells/ml) was treated with VH (0.02% dimethyl sulfoxide) and T0070907 (100 nM and 1 and 5 μM) (A) or GW9662 (100 nM and 1 and 5 μM) (B) at 60 s and VH (0.1% EtOH) and 15d-PGJ_2-G (C) at 135 s followed by PMA/I_o (40 nM/0.5 μM) at 210 s, and the $[Ca^{2+}]_i$ was measured up to 360 s. $[Ca^{2+}]_i$ changes are presented as the ratio intensity of Fluo3/Fura Red versus time. The calcium traces are representative of three independent experiments.

Acknowledgments

We thank Robert Crawford for technical assistance with flow cytometry and Kimberly Hambleton for administrative assistance with the preparation of the manuscript.

Authorship Contributions

Participated in research design: Raman, Kaplan, and Kaminski.
Conducted experiments: Raman.
Performed data analysis: Raman.
Wrote or contributed to the writing of the manuscript: Raman, Kaplan, and Kaminski.

References

Badran BM, Wolinsky SM, Burny A, and Willard-Gallo KE (2002) Identification of three NFAT binding motifs in the 5′-upstream region of the human CD3γ gene that differentially bind NFATc1, NFATc2, and NF-κB p50. *J Biol Chem* **277:** 47136–47148.
Berdyshev EV (2005) *Endocannabinoids in Inflammation and Immune Response.* CRC Press, Boca Raton, FL.
Clark RB, Bishop-Bailey D, Estrada-Hernandez T, Hla T, Puddington L, and Padula SJ (2000) The nuclear receptor PPAR γ and immunoregulation: PPAR γ mediates inhibition of helper T cell responses. *J Immunol* **164:**1364–1371.
Clipstone NA and Crabtree GR (1992) Identification of calcineurin as a key signalling enzyme in T-lymphocyte activation. *Nature* **357:**695–697.
Crabtree GR and Olson EN (2002) NFAT signaling: choreographing the social lives of cells. *Cell* **109 (Suppl)**:S67–S79.
Cunard R, Ricote M, DiCampli D, Archer DC, Kahn DA, Glass CK, and Kelly CJ

(2002) Regulation of cytokine expression by ligands of peroxisome proliferator activated receptors. *J Immunol* **168:**2795–2802.
Feng J, Tamaskovic R, Yang Z, Brazil DP, Merlo A, Hess D, and Hemmings BA (2004) Stabilization of Mdm2 via decreased ubiquitination is mediated by protein kinase B/Akt-dependent phosphorylation. *J Biol Chem* **279:**35510–35517.
Glass CK and Rosenfeld MG (2000) The coregulator exchange in transcriptional functions of nuclear receptors. *Genes Dev* **14:**121–141.
Hauser S, Adelmant G, Sarraf P, Wright HM, Mueller E, and Spiegelman BM (2000) Degradation of the peroxisome proliferator-activated receptor γ is linked to ligand-dependent activation. *J Biol Chem* **275:**18527–18533.
Heppner TJ, Bonev AD, Eckman DM, Gomez MF, Petkov GV, and Nelson MT (2005) Novel PPARγ agonists GI 262570, GW 7845, GW 1929, and pioglitazone decrease calcium channel function and myogenic tone in rat mesenteric arteries. *Pharmacology* **73:**15–22.
Institute of Laboratory Animal Resources (1996) *Guide for the Care and Use of Laboratory Animals*, 7th ed. Institute of Laboratory Animal Resources, Commission on Life Sciences, National Research Council, Washington, DC.
Kanunfre CC, da Silva Freitas JJ, Pompéia C, Gonçalves de Almeida DC, Cury-Boaventura MF, Verlengia R, and Curi R (2004) Ciglitizone and 15d PGJ2 induce apoptosis in Jurkat and Raji cells. *Int Immunopharmacol* **4:**1171–1185.
Klotz L, Dani I, Edenhofer F, Nolden L, Evert B, Paul B, Kolanus W, Klockgether T, Knolle P, and Diehl L (2007) Peroxisome proliferator-activated receptor γ control of dendritic cell function contributes to development of $CD4^+$ T cell anergy. *J Immunol* **178:**2122–2131.
Lee M, Yang KH, and Kaminski NE (1995) Effects of putative cannabinoid receptor ligands, anandamide and 2-arachidonyl-glycerol, on immune function in B6C3F1 mouse splenocytes. *J Pharmacol Exp Ther* **275:**529–536.
Mechoulam R, Ben-Shabat S, Hanus L, Ligumsky M, Kaminski NE, Schatz AR, Gopher A, Almog S, Martin BR, and Compton DR (1995) Identification of an endogenous 2-monoglyceride, present in canine gut, that binds to cannabinoid receptors. *Biochem Pharmacol* **50:**83–90.
Moraes LA, Spyridon M, Kaiser WJ, Jones CI, Sage T, Atherton RE, and Gibbins JM (2010) Non-genomic effects of PPARγ ligands: inhibition of GPVI-stimulated platelet activation. *J Thromb Haemost* **8:**577–587.
Ouyang Y, Hwang SG, Han SH, and Kaminski NE (1998) Suppression of interleukin-2 by the putative endogenous cannabinoid 2-arachidonyl-glycerol is mediated through down-regulation of the nuclear factor of activated T cells. *Mol Pharmacol* **53:**676–683.
Pancani T, Phelps JT, Searcy JL, Kilgore MW, Chen KC, Porter NM, and Thibault O (2009) Distinct modulation of voltage-gated and ligand-gated Ca^{2+} currents by PPAR-γ agonists in cultured hippocampal neurons. *J Neurochem* **109:**1800–1811.
Pascual G and Glass CK (2006) Nuclear receptors versus inflammation: mechanisms of transrepression. *Trends Endocrinol Metab* **17:**321–327.
Piomelli D (2003) The molecular logic of endocannabinoid signalling. *Nat Rev Neurosci* **4:**873–884.
Raman P, Kaplan BL, Thompson JT, Vanden Heuvel JP, and Kaminski NE (2011) 15-Deoxy-Δ12,14-prostaglandin J2-glycerol ester, a putative metabolite of 2-arachidonyl glycerol, activates peroxisome proliferator activated receptor γ. *Mol Pharmacol* **80:**201–209.
Ricote M, Li AC, Willson TM, Kelly CJ, and Glass CK (1998) The peroxisome proliferator-activated receptor-γ is a negative regulator of macrophage activation. *Nature* **391:**79–82.
Rockwell CE, Snider NT, Thompson JT, Vanden Heuvel JP, and Kaminski NE (2006) Interleukin-2 suppression by 2-arachidonyl glycerol is mediated through peroxisome proliferator-activated receptor γ dependently of cannabinoid receptors 1 and 2. *Mol Pharmacol* **70:**101–111.
Sugiura T, Kondo S, Sukagawa A, Nakane S, Shinoda A, Itoh K, Yamashita A, and Waku K (1995) 2-Arachidonoylglycerol: a possible endogenous cannabinoid receptor ligand in brain. *Biochem Biophys Res Commun* **215:**89–97.
Suzuki K, Bose P, Leong-Quong RY, Fujita DJ, and Riabowol K (2010) REAP: A two minute cell fractionation method. *BMC Res Notes* **3:**294.
Széles L, Töröcsik D, and Nagy L (2007) PPARγ in immunity and inflammation: cell types and diseases. *Biochim Biophys Acta* **1771:**1014–1030.
von Knethen A, Soller M, Tzieply N, Weigert A, Johann AM, Jennewein C, Köhl R, and Brüne B (2007) PPARγ1 attenuates cytosol to membrane translocation of PKCα to desensitize monocytes/macrophages. *J Cell Biol* **176:**681–694.
Yang XY, Wang LH, Chen T, Hodge DR, Resau JH, DaSilva L, and Farrar WL (2000) Activation of human T lymphocytes is inhibited by peroxisome proliferator-activated receptor γ (PPARγ) agonists. PPARγ co-association with transcription factor NFAT. *J Biol Chem* **275:**4541–4544.
Yoeli-Lerner M, Yiu GK, Rabinovitz I, Erhardt P, Jauliac S, and Toker A (2005) Akt blocks breast cancer cell motility and invasion through the transcription factor NFAT. *Mol Cell* **20:**539–550.

Address correspondence to: Dr. Norbert Kaminski, Department of Pharmacology and Toxicology, Michigan State University, 1129 Farm Lane, Room 315, Food Safety and Toxicology Building, East Lansing, MI 48824-1317. E-mail: kamins11@msu.edu